

Bacteriorhodopsin Thin Film Assemblies—Immobilization, Properties, and Applications**

By Jin-An He,* Lynne Samuelson,* Lian Li, Jayant Kumar, and Sukant K. Tripathy*

1. Introduction

Supramolecular assembly of optically active materials into thin film architectures is a topic of current theoretical and experimental interest and of significant practical importance. Many device applications of such materials are based on their fabrication into ordered ultrathin films that possess improved optical functionality compared to the bulk state.^[1,2] At a more fundamental level, preferential orientation can also provide a valuable means of probing the electronic interactions and molecular mechanisms in a material. A number of biological materials with supramolecular architectures have evolved to possess inherent and unique optical properties that are highly desirable. The main limitation in the realization of biological materials for device fabrication, however, has been a lack of appropriate immobilization techniques that can both orient the somewhat fragile protein molecules and prevent them from denaturing. A result of these interests has been the study of more rugged biological systems and the development of new immobilization techniques that meet these requirements and provide a means of probing the biochemical interactions in molecularly assembled thin films.^[3]

Bacteriorhodopsin (bR) is the sole protein that exists in the purple membrane (PM) that is extracted from *Halobac-*

terium salinarium.^[4] Under anaerobic conditions and at high salt concentration (about six times that of sea water), the cell membrane of the bacterium grows large patches of a hexagonal two-dimensional crystalline lattice, which consists of embedded bR trimers in a lipid bilayer, called the PM (see Fig. 1). These extreme brine and high temperature growth conditions of the bacterium, together with the crystalline lattice structure of the PM, have resulted in bR that has exceptional stability against salt, high temperature, photochemical degradation, chemicals, and extreme pH media.^[5] This stability has made bR an excellent candidate biomaterial for the investigation of a number of diverse immobilization and optical studies.

The methods recently used for assembling the PM in the solid state or onto solid supports have included Langmuir-Blodgett (LB) deposition,^[6] electric field sedimentation (EFS),^[7] chemisorption self-assembly,^[8] electrostatic layer-by-layer adsorption (LBL),^[9] antigen-antibody molecular recognition,^[10] sol-gel encapsulation,^[11] and using polymers as immobilizing matrices.^[12] These assembly methods have been successful, in large part, because of the superior stability of the bR. Moreover, many of these assembly methods have also been able to provide preferred organization and tailorability of the bR in the assembly to the property and application of interest. For example, the photoelectric conversion efficiency of a bR film is largely dependent on the degree of orientation of the bR in the film.^[10] For photoelectric device applications, LB, EFS, and LBL methods of immobilization may be used because the bR molecules can be preferentially oriented in the final assemblies. On the other hand, for optical holographic applications, it is more important to prepare thicker bR assemblies rather than ordered ones to obtain sufficient optical absorption.^[13] For these applications polymer matrices or sol-gel encapsulation are the preferred methods of immobilization. This review will first discuss the fundamental structure and photocycle of bR and potential bR-based device applications. Several of the current bR immobilization methods that are targeted towards these applications and their effectiveness will be subsequently presented. Lastly, the still controversial mechanism of differential photoelectric response of bR will be discussed, based upon the most recent experimental developments.

[*] Prof. S. K. Tripathy, Dr. J.-A. He
Center for Advanced Materials
Department of Chemistry
One University Avenue
University of Massachusetts Lowell
Lowell, MA 01854 (USA)

Dr. L. Li, Prof. J. Kumar
Center for Advanced Materials
Department of Physics
University of Massachusetts Lowell
Lowell, MA 01854 (USA)

Dr. L. Samuelson
Materials Science Team
US Army Soldier & Biological Chemical Command
Soldier Systems Center
Natick, MA 01760 (USA)

[**] Financial support from the US Army NRDEC is gratefully acknowledged. Discussions with Prof. Michael Rubner at MIT, Dr. Howard H. Weetall at NIST and Dr. Joseph Akarra at the US Army Soldier & Biological Chemical Command are also acknowledged.

2. Structure and Photocycle of Bacteriorhodopsin

Bacteriorhodopsin is a small heptahelical integral transmembrane protein that contains 248 amino acid residues and a retinal chromophore that functions as a light-driven proton pump in the PM of *H. salinarium*.^[14] The prosthetic chromophore is an all-*trans* retinal that is covalently attached to the single polypeptide chain of bR at the ϵ -amino group of lysine at position 216 via a protonated Schiff base (see Fig. 2). Photoisomerization of the retinal from all-*trans* to a 13-*cis* isomer initiates a photochemical cycle in which a proton is transported from the cytoplasmic side to the extracellular side across the membrane.^[15] The electrochemical potential from the resulting proton gradient is used by *H. salinarium* for adenosine triphosphate (ATP) synthesis and bacterium survival in the harsh natural environment.^[16]

Studies on the fundamental proton transfer mechanism of bR have provided valuable information as to how ion

channels in bR, as well as other transmembrane proteins, form and function. Many spectroscopic studies, in combination with genetic engineering, have been carried out to probe the proton transfer mechanism of bR.^[15,17] These results have shown that in the first step a photon initiates the isomerization of retinal from an all-*trans* to a 13-*cis* conformation with a high quantum efficiency of approximately 0.65. This process then deprotonates the Schiff base, within a picosecond, to form a primary charge displacement state. The subsequent steps are thermal transitions, which are normally divided into several intermediates, referred to as K, L, M, N, and O. The characteristic absorption maxima of these intermediates occurs in the visible range with lifetimes ranging from a microsecond to a millisecond.

The bR molecules, initially excited by photons, subsequently relax from the K state through L, M, N, and O states returning to the primary B state (see Fig. 3). The destination of proton translocation is tightly correlated with the specific intermediates, which are accompanied by the correlative



Sukant K. Tripathy is professor of chemistry and director of the Center for Advanced Materials at the University of Massachusetts Lowell. He received his Ph.D. in macromolecular science from Case Western Reserve University. His research interests broadly span molecular organization and supramolecular assemblies of macromolecules and their electronic and optical property aspects, structural modeling, design, and development to obtain unique properties, demonstrate novel phenomena, and create new applications. He received the Carl S. Marvel Creative Polymer Chemistry Award from the American Chemical Society in 1993 and holds 25 US patents.



Jin-An He obtained his Ph.D. in organic chemistry from the Institute of Photographic Chemistry, Academia Sinica (Beijing, China), in 1996 for his work on photochemical and photophysical properties of phycobilin protein assemblies under the supervision of Professor Li-Jin Jiang. He is a research associate at the Center for Advanced Materials at the University of Massachusetts Lowell. His research interests are currently focused on the optoelectronic properties of biological and organic materials, and their assembly chemistry.



Lynne Samuelson was a staff chemist at GTE Laboratories in Waltham, Massachusetts from 1981 to 1987, where she carried out research on the synthesis and molecular assembly of optically active polydiacetylenes and electrically conducting polymers. In 1990 she gained her Ph.D. from the University of Massachusetts Lowell for work on the Langmuir-Blodgett assembly of novel electrically and optically active polymers. At present she is a research chemist in the Materials Science Team at the US Army Soldier Systems Center and an adjunct Professor at the University of Massachusetts Lowell, where she focuses on enzymatically synthesized polymeric materials and the molecular assembly of biological systems for electrical and optical device applications.

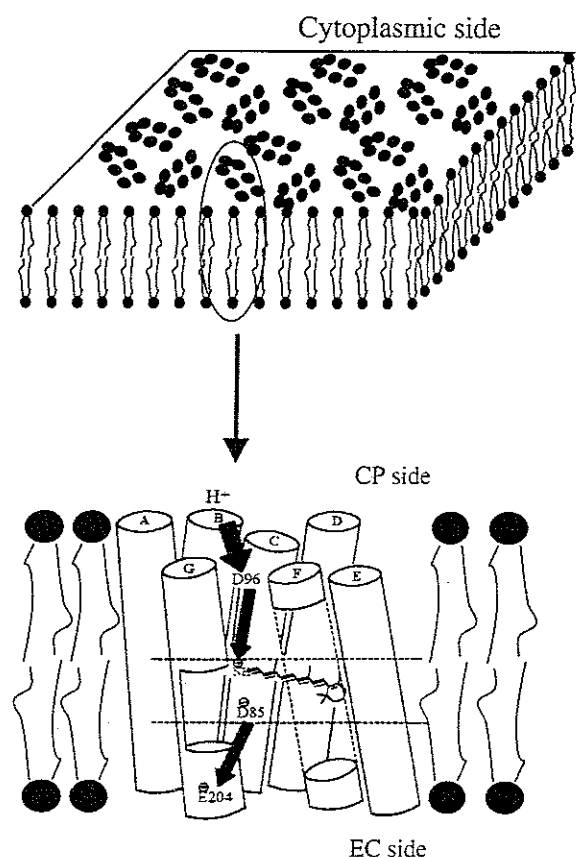


Fig. 1. Structure of the hexagonal crystalline lattice of the purple membrane containing bR trimer units. The secondary conformation of bR monomer shows that seven α -helices span the lipid bilayer. One possible pathway of proton translocation after retinal photoisomerization is indicated by bold arrows (lower part) [18]. The two dotted lines schematically divide bR into three functional regions: top, proton uptake domain; middle, proton exchange domain; bottom, proton release domain.

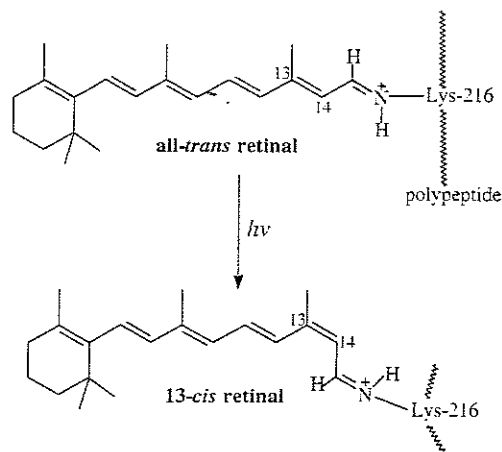


Fig. 2. Photoisomerization of retinal from all-*trans* to 13-*cis* in bR. Under illumination by visible light, the light-adapted bR containing 100% all-*trans* retinal is isomerized to the 13-*cis* conformation around the C₁₃-C₁₄ bond to initiate the complicated photocycle of bR.

protein conformational change. Thus, the photocycle of bR underpins reversible photochromic behavior as well as charge displacement. The trajectory of the proton transfer in bR has been followed more clearly using site-specific

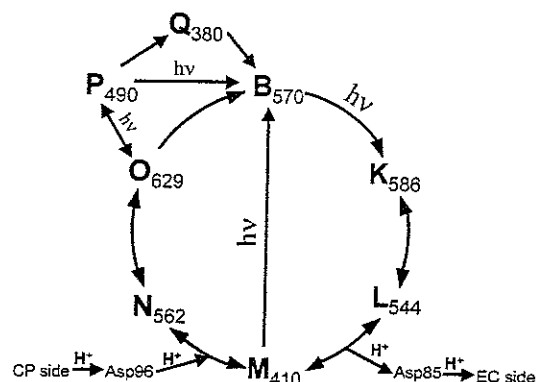


Fig. 3. Simplified illustration of the photocycle of bR. The intermediates of bR are shown by a single letter and their absorption maxima are given as subscripts [46]. A branched Q state is the stable intermediate containing 9-*cis* retinal for photochromic applications [24]. As shown, the uptake and release of protons is tightly correlated to the decay and formation of the M state in the bR photocycle.

mutagenesis of bR in combination with recent X-ray diffraction studies. However, the exact mechanism of the proton channel is still unclear and is currently explained using various models.^[18] Generally, the Schiff base, hydrogen bond network (formed by several water molecules along the route of proton translocation), and amino acid residues Asp85 and Asp96 (Asp stands for aspartic acid) are involved in the formation of the proton channel. The model most widely accepted today involves deprotonation of the Schiff base and transfer of a proton to Asp85, which subsequently releases the proton to the extracellular side in the L to M reaction. The deprotonated retinal chromophore then takes up a proton from Asp96, which subsequently regains a proton from the cytoplasmic side in the M to N reaction. The proton release precedes proton uptake at neutral and high pH, and the sequence is reversed and proton uptake is followed by proton release at low pH.^[19]

Unlike typical biological materials, PM has high thermal and photochemical stability. Bacteriorhodopsin can retain its natural structure and function to temperatures as high as 140 °C in the dry state and for pH ranging from 3 to 10 in solution.^[5] The proton-pumping photocycle of bR can be repeatedly cycled more than 10⁶ times.^[20] This unusual stability, coupled with its unique photochemical and photophysical properties, has made bR the most promising biological material for device applications.

3. Potential Applications of bR

Proposed technical applications of bR can be grouped into four general categories, based on the physiological functions and properties utilized. These are energy conversion, applications in optoelectronics, optical storage and information processing, and nonlinear optics.

Bacteriorhodopsin is a simple yet integral photosynthesis reaction center in the archaebacterium *H. salinarium*, the first application involves its use as an energy conversion system

to transform light energy into electrochemical energy. A solar energy cell with a conversion yield of 0.5 % using bR has been reported by Caplan and Fischer.^[21]

A second application involves exploiting the different photovoltage and photocurrent responses of bR at the various time scales that arise from the charge displacement and proton translocation.^[10,22] These photoelectric signals can be extracted into optoelectronic device applications. One example is a pixel network of small bR photoelectric cells fabricated by Miyasaka and co-workers for the purpose of image detection.^[23]

The third application involves the use of the photochromic properties of the bR, where absorption of a photon leads to reversible photochemical and thermal cycles. Several intermediates, each with different absorption wavelengths and lifetimes, have been identified in the photocycle of bR. At present, the M and Q states are the most promising intermediates for photochromic applications since these two intermediates show the most obvious spectral shifts and longest lifetimes (see Fig. 3). Through excitation at different wavelengths, the bR can be reversibly converted between the M or Q intermediate and the primary B state.^[24] This behavior makes bR attractive for optical information processing and storage. The optical and holographic applications of bR solid films have been described in a review by Oesterhelt and co-workers.^[25]

The last application involves the use of the retinal of bR. The retinal is a conjugated polyene chromophore whose extended π -electron system exhibits large second-order and third-order polarizabilities as measured by second-harmonic generation and two-photon absorption, respectively.^[26] The inherent structure of the hexagonal two-dimensional crystalline lattice of the PM forces the retinal into an orderly array in a PM fragment. In addition, it has been demonstrated that PM fragments themselves may be oriented using EFS and LBL assembly methods. This added degree of orientation of the retinal further enhances the nonlinear optical (NLO) susceptibility of bR assemblies for NLO applications.^[25,26]

A more fundamental application includes investigation and optimization of the mechanism of the proton channel using genetically engineered site-mutated bRs.^[27] These mutants have significantly different properties than the wild-type bR. These differences include new spectral shifts and lifetimes of intermediates, modified photocycles, and in some cases improved properties for device applications. For example, in the D96N mutant, the Asp96 is replaced by asparagine in which the second carboxyl group is substituted by a carboxyamido group. This mutation of a single amino acid changes the source of reprotonation of Schiff base from Asp96 to the local medium, and results in a change in the lifetime of the M intermediate. This change in the M lifetime results in unique optical and photoelectric properties.^[24,25] Thus, genetic engineering of bR is a powerful method both to investigate the fundamental mechanisms of the proton channel and to design and optimize bR properties for device applications.

4. Immobilization of Bacteriorhodopsin

A primary method used for the molecular level arrangement of materials is LB deposition.^[2] In this method, amphiphilic molecules are first spread at an air-water interface, compressed and oriented, and then deposited into multilayer assemblies. Until recently, this method was the preferred technique to prepare highly oriented molecular films. However, not all molecules, in particular water-soluble proteins, can be easily processed into ordered multilayers using this technique. Generally, only molecules that are amphiphilic and water insoluble may be used. Therefore, other physical and chemical assembly techniques have been developed to overcome these limitations and form ordered assemblies of less-traditional materials.^[28] Versatile molecular self-assembly techniques that utilize chemical bonding, hydrogen bonding, van der Waals forces, coulombic electrostatic interactions, and hydrophobic/hydrophilic affinity have become very effective methods for fabricating organized solid films.^[1] These techniques are simple, versatile, and can be used under very mild conditions, making them suitable for immobilization of more fragile biological materials. The next section will discuss and compare the use of several of these techniques for the assembly of bR thin films.

4.1. LB Technique

LB is the method of choice for the formation of highly ordered, ultrathin films of organic, amphiphilic molecules. Extension of this technique to form ordered films of PM fragments occurred over twenty years ago.^[29] However, the LB technique had to be appropriately modified to compensate for the more sensitive PM fragments (bR protein and lipids), which were known to denature when placed in most organic solvents. These concerns led to the use of mixed (hexane or dimethylformamide) and water solvent systems to preserve the PM and the addition of extraneous lipids such as soya-phospholipid to improve the homogeneity of the films.^[6]

The PM fragments are known to be approximately 0.5–2 μm in size and about 5 nm in thickness.^[30] Through these studies it was found that, at the air/water interface, the cytoplasmic (CP) side of the PM is more hydrophilic than the extracellular (EC) side.^[31] Therefore, it was expected that the CP side would be the preferred side to face the subphase during Langmuir monolayer formation (see Fig. 4). Early studies showed that approximately 85 % of the PM fragments were oriented in the same direction in the LB films.^[29] However, further detailed studies using immunogold labeling and electron microscopy indicated that the surface orientation of the PM is substantially random in the films.^[32]

In order to improve the orientation of the PM in LB films, Koyama and co-workers established a method using bispecific antibodies that could simultaneously recognize both a phospholipid hapten and a specific side of the bR

molecule.^[10] Here it was found that by using the phospholipid hapten as a monolayer template at the air-water interface, over 85 % orientation of the bR could be achieved. The highly ordered PM films could be prepared by the antigen/antibody molecular interaction and subsequently transferred onto solid supports using the LB method. The photoelectric cells fabricated from these types of films showed significantly improved photoelectric response, confirming that improved orientation of the PM had been achieved.^[10]

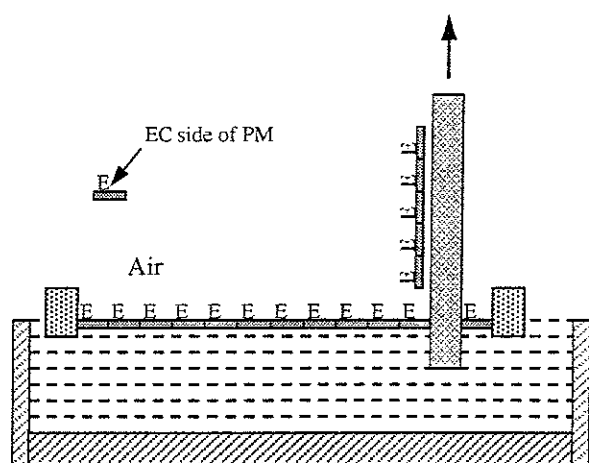


Fig. 4. Scheme for the preparation of the PM film by the LB technique. Since the CP side of the PM is more hydrophilic than the EC side, it is proposed that the CP side has a preferred orientation facing the subphase at the air/water interface [31]. However, experimental evidence shows that the degree of orientation of the PM in its LB film is not as high as expected due to the interference of other molecular interactions [32].

Over the years, these types of studies have shown that it is possible to prepare oriented LB films that have a high degree of bR orientation and good optical response. However, the time-consuming procedures necessary to prepare thick films (PM is only 5 nm thick) and the requisite complicated modifications of the technique to bR has limited its use for practical device fabrication.

4.2. Electric Field Sedimentation

PM fragments, like many other biological membranes, have a net negative charge on both sides of the membrane. These charges are due to amino acid residues on the surface of the bR, the C-terminal and N-terminal of the polypeptide chain, and intrinsically acidic lipids.^[33] Jonas and co-workers have provided a detailed review on the surface charge properties of the PM.^[34] In general however, it is difficult to determine precisely the surface charge density of PM fragments because of the unknown distribution of lipids surrounding the bR and the presence of cationic effects with a local pH. Several different methods that use the Gouy-Chapman theory have been reported to measure the surface charge density of PM, but the results are inconsistent and span

a range from 0.5 to 9 negative charges per bR.^[34] The most consistent results indicate that the surface charge density at pH 6.6 is more negative on the CP side (-2.5 charges/bR) than on the EC side (-1.8 charges/bR).^[35] The generally accepted opinion is that the PM is always negatively charged, and the CP side is more negative than the EC side at > pH 5 and vice versa at < pH 5.^[34] This charge asymmetry of the PM results in a permanent dipole moment directed from the CP side to the EC side.^[36]

Since the PM is known to have a net electric dipole moment, addition of an external electric field to an aqueous PM solution results in the orientation of the PM fragments in the direction of the electric field. Furthermore, if two electrodes are inserted into a PM suspension and then an electric field of 20–30 V/cm is applied, the PM fragments will electrophoretically move (because of the net negative charge), sediment onto the cathode, and form an oriented PM film.^[7] This method is simple, quick, and effective for the fabrication of oriented PM films. In addition, control over which side of the PM (EC or CP) faces the electrode may be obtained through simple adjustment of the pH of the PM suspension.^[37] Figure 5 illustrates the standard setup for preparing an oriented PM film by the EFS technique. Typically the thickness of the film is dependent on the time of the applied DC electric field; a 10 μm thick film can be obtained by application of a 20–30 V/cm DC electric field for about 1 min.

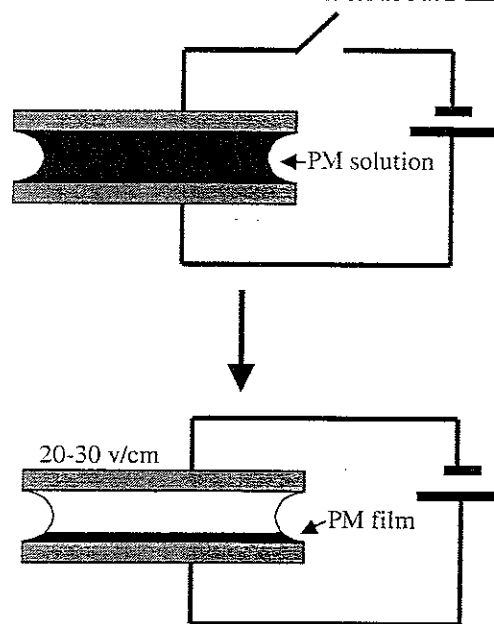


Fig. 5. Setup for the fabrication of oriented PM films by the electric field sedimentation method. Due to the net negative charge of the PM, the PM fragments will move and attach to the cathode to form a dense PM film.

4.3. Immobilizing Matrices and Sol-Gel Encapsulation

A modification of EFS has included encapsulation into a polymer gel in combination with orientation by an electric field to obtain oriented PM-containing solid films.^[38] In this case, PM fragments were embedded into either poly(vinyl

alcohol) or polyacrylamide gels, while an electric field was applied to orient the PM during the setting period. Once the gel has set, the PM is immobilized and locked into the preferred orientation. Researchers have also shown that bR can be immobilized into optically clear sol-gel glass and still maintain its physiological and photochemical activity.^[11] The sol-gel process involves the hydrolysis and condensation polymerization of alkylsilicate and alkoxyalkylsilane materials to produce a transparent glass under mild conditions. The observed lifetime increase of the M intermediate of bR in the sol-gel glass makes this system attractive for photochromic applications.^[11]

4.4. Electrostatic LBL Self-Assembly Technique

The area of thin film formation and self-assembly has been greatly impacted by the recent development of the LBL electrostatic self-assembly method. This technique is extremely simple, versatile, and effective for the assembly of oppositely charged species onto solid supports.^[39] The LBL approach was first utilized by Decher and co-workers,^[40] with the alternate layering of oppositely charged polyelectrolytes, and by Rubner,^[41] with the electrostatic layering of conducting polymers. In LBL assembly, spontaneous sequential adsorption of polycations and polyanions is carried out from dilute aqueous solutions onto charged surfaces. The technique is extremely versatile as the structure, components, and thickness of the films can be controlled through judicious choice of electrolytes and processing conditions. The LBL technique is based on the strong electrostatic interaction between oppositely charged polyelectrolytes. Typically, a charged solid support is immersed into an oppositely charged polyanion solution. Electrostatic attraction occurs between the charged surface and the oppositely charged molecule in solution. If the concentration of polyanions is sufficient, adsorption occurs until there is a complete charge reversal at the solid support surface. After being rinsed in water, the support is then exposed to a solution of the oppositely charged polyanion and the process is repeated until the desired number of layers is achieved. In this adsorption technique, the main concern is to make sure that complete charge reversal occurs after each deposition into the polymer solutions in order to obtain continuous and homogeneous multilayer film formation.

The LBL method has since been extended to a wide variety of other interesting charged materials, including dendrimers, azo polymers, poly(*p*-phenylenevinylene) (PPV, a polymer used in light-emitting diodes),^[42] metal and semiconductor nanoparticles, organic microcrystals,^[43] and inorganic and organic materials.^[44] LBL has even proven to be quite effective for the layering of biomaterials such as proteins, enzymes, DNA, and viruses.^[45] The LBL method is desirable largely because of its versatility: it can be used to produce layers of virtually any charged material under the right conditions. In the case of biomaterials, the LBL method is

also advantageous because the conditions of deposition may be altered to specifically protect the biofunctionality of the material of interest.

As mentioned previously, PM fragments are known to have an asymmetric, negatively charged surface, where the CP side contains more negative charges than the EC side at pH values above 5.^[34,35] This type of structure makes PM very suitable for layering using the LBL method. In addition, it appears that the asymmetry of the PM also provides for a high degree of orientation of the PM, similar to what is obtained using the EFS method.^[9] Since an external electric field is not required, LBL deposition is a milder and more facile method for the fabrication of oriented PM assemblies.

A typical LBL adsorption process for the preparation of polycation/PM multilayers is illustrated in Figure 6. Here, an aqueous solution of commercially available poly(diallyldimethylammonium chloride) (PDAC) of medium molecular weight, 2.0 mg/mL containing 0.5 M NaCl, pH 6.8, was used as the polycation solution. The polyanionic PM suspension was made from a pH 9.4 solution with a concentration of 0.5 mg/mL of bR (1.2 optical density in a 1 cm cuvette at 570 nm calculated according to $\epsilon = 63\,000\text{ M}^{-1}\text{ cm}^{-1}$ and molecular weight MW = 26 000).^[46] A solid support with a negatively charged planar surface was first immersed in the PDAC solution for 5 min until a homogeneous polycation monolayer was adsorbed. After being rinsed in Milli-Q water for 2 min and dried with N₂, the modified support was then transferred into the PM suspension (pH 9.4) for 5 min, rinsed with water (pH 9.4) for 2 min and again dried by N₂. This process was repeated until the desired number of bilayers of PDAC/PM was obtained.

In order to obtain homogeneous and reproducible growth of each PM monolayer within the PM/PDAC assemblies, the pH of the PM solution and the adsorption time of the support in the PM solution must be stringently controlled. Based on our results,^[9] the amount of adsorbed PM increases with the pH of the PM solution. A pH of 9.4 was found to provide sufficient coverage of the PM to render the surface negatively charged so that the subsequent layer adsorption process may be continued. A possible explanation of this pH effect is that there are several competing molecular interactions that can occur between the PM and PDAC, which can cause aggregation and spontaneous assembly. These molecular interactions include hydrophobic/hydrophilic interactions, hydrogen bonding, van der Waals forces, and coulombic electrostatic interaction. Therefore, it is reasonable to believe that these also participate in the adsorption process between the PM and PDAC under certain conditions. However, when the negative charge density of the PM is large enough, as it would be at high pH, these other molecular forces are minimized and electrostatic interaction becomes the dominant driving force in the adsorption process. It was found that in acidic and neutral medium, a smaller amount of PM was adsorbed with each layer and adsorption eventually stopped after several layers. This is further evidence that other molecular interactions can

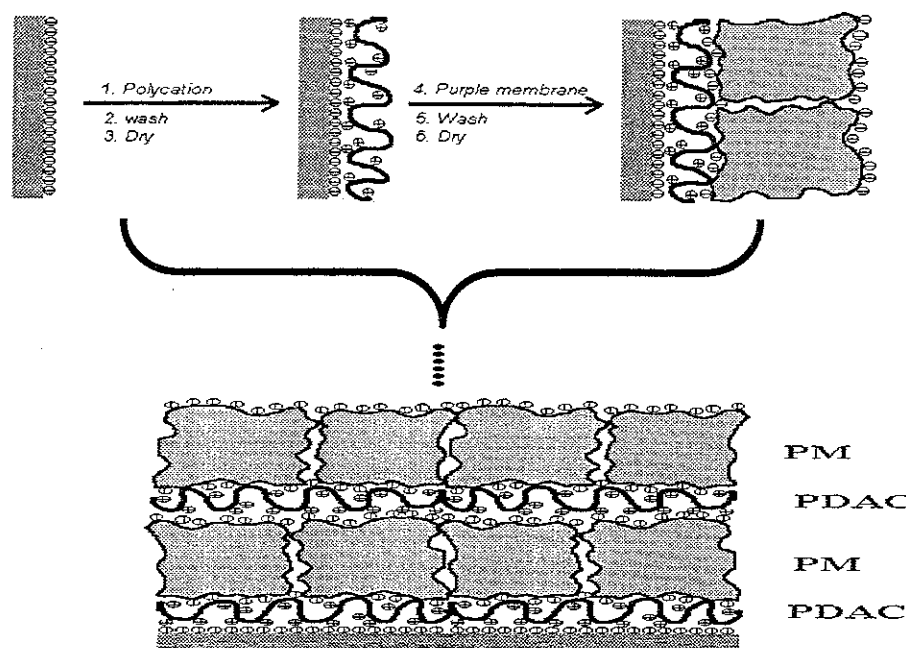


Fig. 6. Schematic diagram of the PDAC/PM LBL adsorption. As shown, a layer of the polycation, PDAC, is first adsorbed onto the pretreated negatively charged surface of the solid support. Subsequently, a monolayer of the polyanion, bR, is electrostatically adsorbed onto the PDAC layer by control of the adsorption time and pH. A PDAC/PM multilayer can be easily obtained by the LBL method by repeating the above procedure.

hinder and interfere with the preferred coulombic forces that are needed for electrostatic adsorption. This type of aggregation behavior has also been observed in LBL film formation with other materials.^[47] Once aggregation occurs, film growth becomes random and inhomogeneous and eventually results in a very poor degree of orientation and percentage deposition.

Once the pH conditions of PM suspension were optimized, a correlation of the amount of PM adsorption with time could be determined. It was found that after 5 min adsorption time a homogeneous monolayer of PM was deposited onto the PDAC layer. However, when the adsorption time was increased to 10 min, aggregation of the PM occurred and an additional monolayer of PM deposited onto the PDAC preadsorbed surface.^[9] The reproducibility of the PDAC/PM multilayer growth was determined by measuring the spectral absorption change with each bilayer. Figure 7a shows the UV-vis absorption spectra for the sequential deposition of PDAC/PM bilayers at each consecutive step of the multilayer assembly process. As shown, the multilayer growth of the PDAC/PM assemblies is linear and reproducible. The characteristic absorption peaks for bR at 278 and 563 nm are observed to increase proportionally with each additional bilayer as shown in Figure 7b. This is further evidence that the electrostatic deposition is a linear process and that each transfer contributes an equal number of PM fragments to the film assembly once the conditions are optimized.

The UV-vis data also show that the deposited PM fragments in the PDAC/PM multilayers are not denatured, as the characteristic absorption bands of the PM are still

present. There is, however, a slight blue shift of about 5 nm for the peak at 563 nm compared to the absorption of the PM in solution. A similar blue shift in a dried PM film was previously observed with a bR/soy-l- α -phosphatidylcholine LB film.^[6] This behavior was explained by the dehydration of the Schiff base of the retinal chromophore in bR in the absence of water, while, in the presence of water, the proton Schiff base is localized and a red shift is observed.^[51]

The absorbance of each deposited bilayer of PDAC/PM was calculated to be 1.5×10^{-3} at 563 nm from the slope of the line shown in Figure 7b. This absorbance is due to the PM only, since PDAC contributes no absorption in this range. It is interesting to compare this value with that of bR/soya-PC LB films. In the LB films, the absorbance of a bR monolayer is approximately 0.32×10^{-3} to 0.45×10^{-3} at 570 nm,

depending on the weight ratio of bR to soya-PC and the deposition pressure of the film.^[6] The absorbance of the LBL-assembled films, however, is roughly 3–5 times higher than that observed with the LB films. This result suggests that the PM fragment assemblies prepared using this spontaneous LBL assembly may be organized into more compact, dense monolayer formations. In contrast, soya-phospholipid must occupy part of the area in the bR/soya-PC LB film and this dilution effect leads to the decrease of the absorbance of the bR monolayer. This improved packing and organization of the PM in these films offers some advantages over previous bR films for device fabrication, because the sensitivity and performance of the devices depends greatly on the amount and orientation of the bR in two-dimensional configurations.

Characterization of the uniformity of the PDAC/PM assemblies was carried out using ellipsometry and atomic force microscopy (AFM).^[9] Ellipsometry showed an average thickness of 55 Å for a PDAC/PM bilayer. This value is in good agreement with the known thickness of PM (approximately 50 Å) and the known thickness of a PDAC monolayer (5–10 Å). AFM provided further detailed information involving the surface morphology and the homogeneity of the PM film down to the nanometer scale. Figure 8 shows an AFM image of one bilayer of PDAC/PM with PM as the outer layer. Electrostatic adsorption of PM on the PDAC surface results in the formation of a monolayer of PM, as shown by the large patches dispersed across the surface. The cross-sectional analysis indicated that the thickness of a large patch is about 55 Å and this value was found to increase to

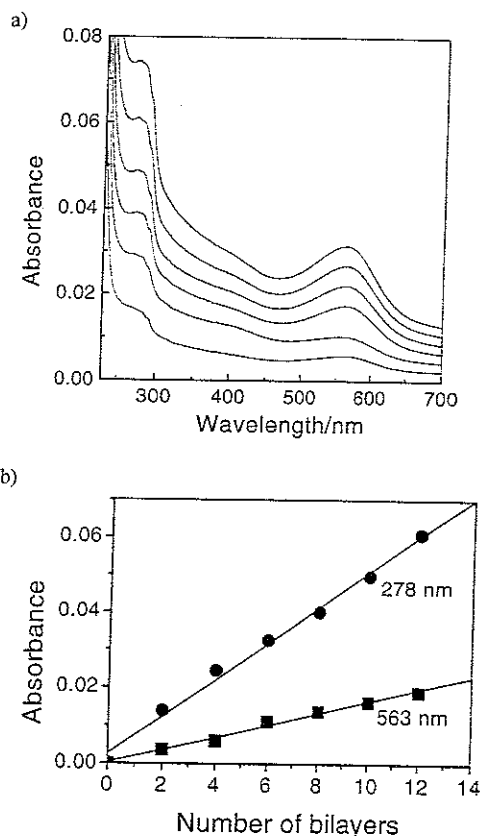


Fig. 7. a) UV-vis absorption spectra of alternately adsorbed PDAC/PM multilayers. The curves, from bottom to top, correspond to adsorption of 2, 4, 6, 8, 10, and 12 alternate PDAC/PM bilayers, respectively. b) Increase of the absorption at 278 and 563 nm with the number of bilayers. The baseline increase is due to light scattering of the PDAC/PM multilayers; its contribution was deduced from the total absorbance.

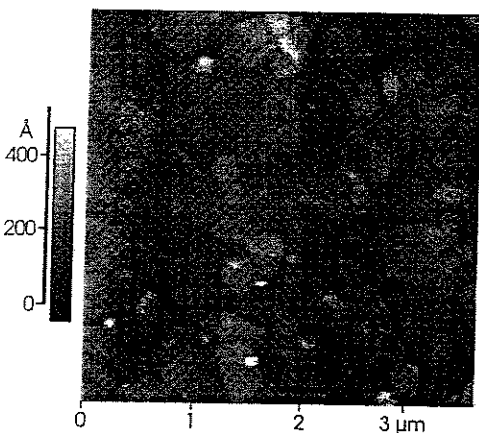


Fig. 8. AFM image of one bilayer of the PDAC/PM film with PM as the outer layer.

110 Å at the boundary of two patches of PM, most likely due to their partial overlap. These results confirmed that organized monolayers of the PM are, in fact, obtained within the PDAC/PM bilayers and that the final thickness of the PDAC/PM assemblies may be controlled by simply repeating the layer-by-layer adsorption as desired.

The second-order NLO susceptibility of the PDAC/PM multilayer assemblies was measured by second harmonic generation (SHG) to determine the degree of orientation of the PM. The NLO properties of the PM fragments have been investigated and it was determined that the retinal chromophore of bR exhibits an extremely large second-order polarizability due to the conjugated polyene π -electron structure and its acentric arrangement due to the polypeptide and the crystalline lattice.^[26] The higher the degree of orientation of the PM in the films, the larger the NLO coefficient becomes. The relationship between the transmitted second harmonic intensity of the double-sided multilayers (PDAC/PM films deposited on both sides of the glass slide) and the incident angle is shown in Figure 9. The interference pattern arises from the phase difference between the SH waves generated at each side of the glass during propagation of the fundamental wave. Complete extinction appeared for destructive interference over the whole film and this indicated that the PDAC/PM multilayers deposited on both sides of the glass slide are uniform.^[48] To evaluate the degree of PM orientation in PDAC/PM multilayers, the magnitude of second-order susceptibility in this film was compared with that known for electric-field-oriented PM films. The second-order susceptibility $\chi^{(2)}$ of the PDAC/PM films (12 bilayers) was measured and determined to be 8.1×10^{-9} esu by a SHG technique.^[9] This value is somewhat larger than that obtained with an electrophoretically sedimented film of bR (5.4×10^{-9} esu),^[49] and indicates that the degree of order of the PM fragments in the PDAC/PM multilayers is as good as, if not better than that obtained using EFS. Since the CP side of the PM is known to contain more negative charges than that of the EC side under alkaline conditions,^[35] it is expected that, in LBL deposition, the CP side of the PM is preferentially drawn to and adsorbed on the polycationic PDAC layers.

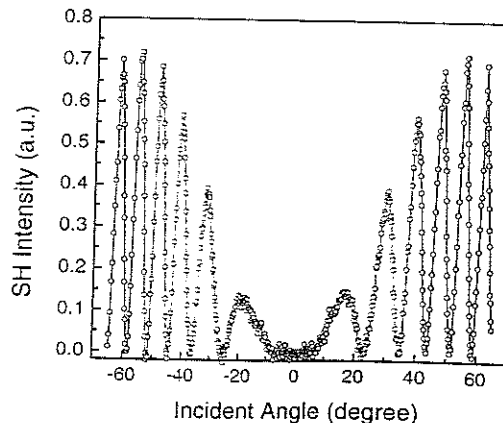


Fig. 9. Second-harmonic intensity as a function of incident angle of the fundamental laser beam from a double-sided LBL self-assembled PDAC/PM multilayer (12 layers).

This LBL electrostatic deposition technique appears to offer several advantages for the preparation of organized thin films of bR compared to other established techniques

such as LB and EFS methods. One major advantage is that the LBL technique is milder than the other methods. In LBL no organic solvents or external fields, which can cause the denaturation of the PM, are required. In addition, the LBL method is extremely facile in that no specialized equipment, modified chemicals, or time-consuming preparation or procedures are required. An oriented PDAC/PM bilayer can be prepared on the benchtop, using only a few aqueous solutions in beakers and 15 min of time. Another advantage is the versatility of this technique to integrate bR with other interesting systems. Since this approach has already been applied to a variety of charged molecules such as conducting polymers, nanoparticles, enzymes, and proteins,^[41-45] it is reasonable to believe that these types of molecules could also be easily intercalated with bR either to enhance bR properties or to add additional functionality to the final assemblies for a host of potential optoelectronic applications.

5. Differential Photoelectric Response of PDAC/PM Multilayers

Photoelectric studies of the PM, especially the transient photoelectric signals from the charge separation and displacement after the photoexcitation of bR, have provided fruitful information for understanding the molecular mechanism of the bR proton pump.^[22] On the nano- and microsecond time scales, two fast photoelectric components, referred to as B1 and B2, were observed by flash photolysis. The negative polarity component B1, with a rise time of less than 1 μ s, is believed to be associated with the initial proton pumping event, i.e., the charge separation as a result of the light-induced retinal isomerization from all-*trans* to 13-*cis* in bR.^[50] The positive polarity component B2 on the microsecond time scale is due to the vectorial pumping of protons from the Schiff base to solution.^[51] On the millisecond time scale, a pH-dependent component B3 was observed but its origin is not clear.^[52] The differential photocurrent components D1 (light-on component) and D2 (light-off component) from bR under continuous green light excitation is an important and desirable property for electronic device applications. Moreover, the magnitude and efficiency of the differential photocurrents that can be generated from bR films is quite dependent on the effectiveness of a bR layering technique.^[10,23]

However, there are conflicting opinions regarding the actual molecular mechanism of the differential photocurrent (D1 and D2). Miyasaka and co-workers have suggested that the charge displacement within bR induces the differential current on the electrode adjacent to the bR molecule when bR is excited by light.^[10] Robertson and Lukashev, however, have reported that the differential current of bR results from an electrochemical current induced by the local pH change and not by charge displacement.^[53] More recent, strong experimental evidence from El-Sayed and co-workers

supports the latter conclusion.^[37] In their work, through comparative studies carried out under both pulsed and continuous wave (CW) laser photoexcitations on different time scales, an identical polarity change with pH was found for the slow B3 photocurrent component under pulsed laser excitation and the D1 differential current component from CW laser excitation. Therefore, the origin of the D1 photocurrent should be the same as for B3. Since the B3 component results from the proton accumulation near the electrode/bR interface, the D1 was inferred to come from the change of proton concentration at the electrode/electrolyte interface as a result of the proton pumping of bR. This leads to the formation of a transient proton capacitor between the working and counter electrodes. The charging and discharging processes of the proton capacitor produce the differential photoelectric response of bR.

To further understand the origin of the differential photocurrent of bR, the photoelectric responses from the multilayers of the wild-type PM (WT-PM) and the D96N mutant prepared by the LBL technique were measured using the liquid-junction photocell configuration. The differential photoelectric responses for eight bilayers of PDAC/WT-PM ((PDAC/WT-PM)₈) and six bilayers of PDAC/D96N ((PDAC/D96N)₆) are given in Figures 10a and 10b, respectively. Figures 10c and d show the dependence of the magnitude of the light-on photocurrents on the number of bilayers in the PDAC/bR assemblies. It is observed that the WT-PM and D96N mutants generate substantial differential currents, which indicates that the physiological activity of bR in both of these systems is preserved after electrostatic deposition. The differential response properties of these currents are in excellent agreement with those previously obtained using other layering techniques.^[6,10] Figures 10c and d show that a maximum light-on current of 52 nA/cm² for (PDAC/WT-PM)₈ and 80 nA/cm² for (PDAC/D96N)₆ are observed. These results indicate that the photoelectric sensitivity of the D96N mutant is higher than that of the WT-PM since a larger photoelectric response is observed with the thinner D96N assembly. Also, it has been shown that films containing the D96N mutant show an improved holographic diffraction efficiency compared to WT-PM films.^[24] These results show that genetic engineering is a useful technique to modify and tailor the photochemical and photophysical properties of bR for improved application performance.

It is also important to note in Figure 10 that the ratio of the magnitude of the light-on/light-off photocurrent from the WT-PM assembly (approximately 1.2) is much smaller than that observed for the D96N mutant (approximately 2.8). Also, the time scale (defined from maximum peak current to zero) of the WT-PM (about 500 ms for both the light-on and light-off currents) is significantly smaller than that observed with the D96N mutant (about 3 s for the light-on current and about 6 s for the light-off current). These photoelectric differences between the WT-PM and D96N correspond to amino acid replacement, i.e., the protonatable aspartate at the 96 position in the WT-PM has been substituted by a non-

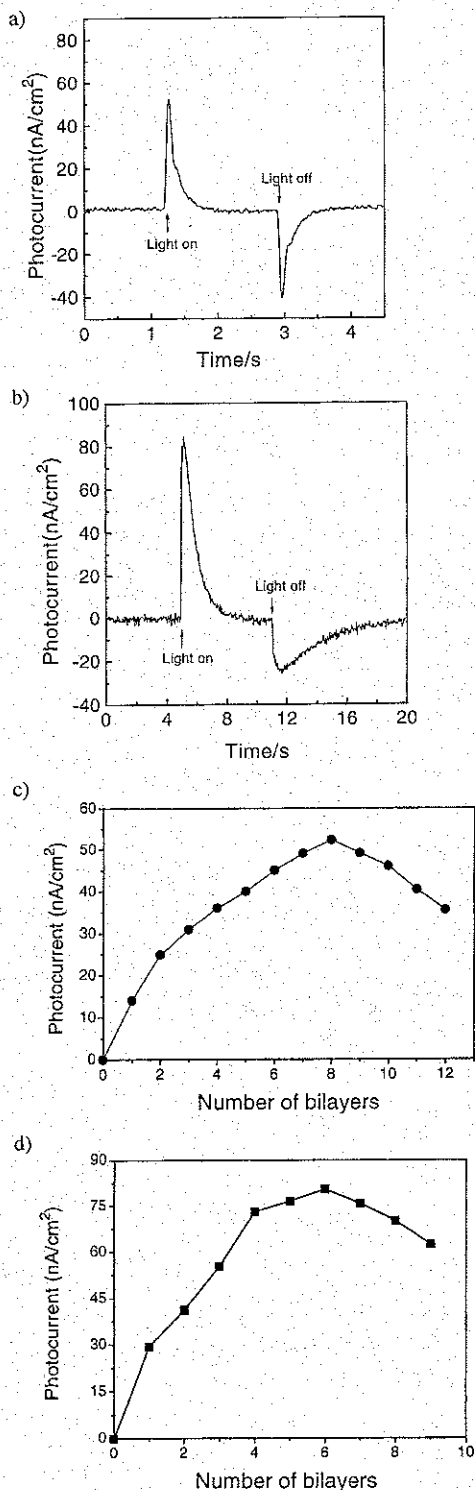


Fig. 10. Typical differential photocurrent from a) (PDAC/WT-PM)₈ and b) (PDAC/D96N)₆ deposited onto ITO electrodes. c, d) The dependence of the magnitude of the light-on photocurrent with the number of bilayers for WT-PM (c) and D96N (d). The electrolyte solution is 0.5 M KCl, pH 8.5 for the WT-PM and pH 7.2 for the D96N mutant.

protonatable asparagine (Asn) in the D96N mutant. This substitution makes the decay rate of the M intermediate in the D96N much slower,^[54] because the deprotonated Schiff

base cannot reprotonate from Asn96 and is forced to obtain the proton from the solution medium only. This creates a barrier for the proton uptake in the D96N mutant and makes the magnitude of the light-off peak much smaller than that of the light-on peak since the light-on photocurrent corresponds to net proton release and the light-off photocurrent relates to net proton uptake.^[53]

To completely clarify the molecular mechanism of differential photocurrent generation of bR, the effect of sodium azide in the electrolyte solution, which can catalyze proton transfer in the WT-PM and recover the kinetic defect in the D96N mutant, was investigated.^[55] With addition of NaN₃ to the electrolyte solution, the magnitudes of the differential photocurrents from the PDAC/WT-PM multilayers roughly double compared with those without NaN₃ in the electrolyte solution.^[9] Here, the effect of azide on the differential photocurrent of bR should not be explained simply as the electrolyte concentration effect (or ionic strength effect)^[37] because studies by LeCoutre and co-workers have shown that this type of increase is expected and is due to the azides ability to catalyze the proton transfer steps, which accelerates M formation and decay by about a factor of two in the WT-PM.^[55] Since M formation (from L to M state) and decay (from M to N state) in the bR photocycle is directly correlated with proton release and uptake, this results in a local net change of proton concentration (see Fig. 3). Therefore, the quantitative relationship between the differential photocurrent and the concentration of NaN₃ indicates that the millisecond differential photocurrent originates from the local pH change, which is due to the change of proton concentration from M formation and decay. The formation of the M intermediate, which leads to an increase of proton concentration at the electrode/electrolyte interface due to proton release of bR, produces the light-on photocurrent; the decay of the M intermediate, which results in a decrease of proton concentration at the interface due to proton uptake of bR, contributes to the light-off photocurrent.

The effect of azide on the differential photocurrent of D96N mutant supports the above view. The dependence of the light-on photocurrent (curve 1) and light-off photocurrent (curve 2) on the concentration of NaN₃ for (PDAC/D96N)₆ films is presented in Figure 11a. Figure 11b shows the ratio of the magnitude of the light-on to light-off peak photocurrent at different concentrations of NaN₃. These results show that the influence of NaN₃ on the photocurrent of D96N mutant is somewhat different from that observed with WT-PM.^[9] First, the magnitudes of both the light-on and light-off photocurrent increase sharply within a narrow concentration range of NaN₃ (< 1.3 mM). This is in accordance with the effect of azide on the photocurrent of WT-PM, and shows that NaN₃ can accelerate the formation and decay of the M intermediate in D96N, resulting in an increasing change of proton concentration at the electrode/electrolyte interface. Second, with increasing concentration of NaN₃, the rate of increase of the light-on photocurrent in

D96N mutant is slower than the rate of increase of the light-off current, as presented in Figure 11b. This behavior may be explained by the well-known capability of NaN_3 not only to catalyze proton transfer in bR, but also to compensate for the kinetic defect of the D96N mutant, which causes a dramatic retardation of the M decay.^[54] As shown previously in Figure 10b, the magnitude of the D96N light-off photocurrent is observed to be significantly smaller than that of the light-on photocurrent because the mutant lacks a proton donor (Asp96) and must take up a proton more slowly from the solution medium. Figure 11b illustrates the effect of this kinetic defect, as a large light-on/light-off ratio is observed at very low concentrations of NaN_3 . On the other hand, as NaN_3 is added, the light-on/light-off ratio rapidly decreases to a constant value of approximately 1.7, showing that the NaN_3 is able to compensate for the mutants lack of a proton donor.

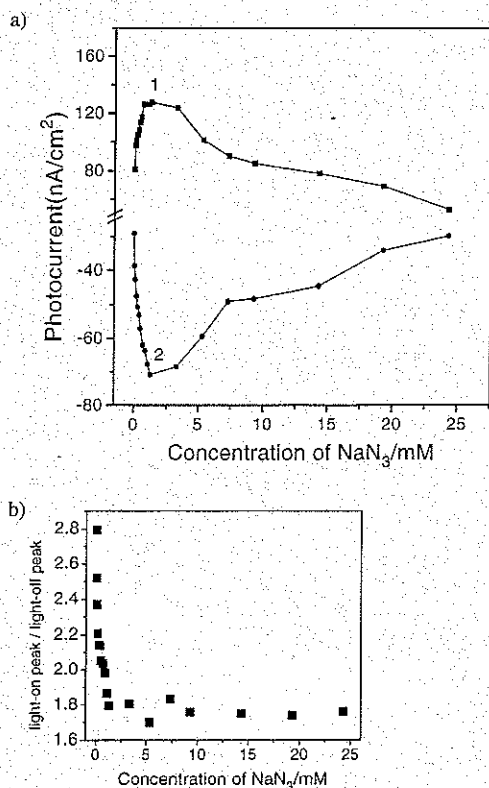


Fig. 11. a) Dependence of the light-on photocurrent (curve 1) and light-off photocurrent (curve 2) for a (PDAC/D96N)₆ film on the concentration of NaN_3 in 0.5 M KCl, pH 7.2 electrolyte solution. b) The ratio of the magnitude of the light-on photocurrent to light-off photocurrent as a function of the concentration of NaN_3 .

6. Conclusions

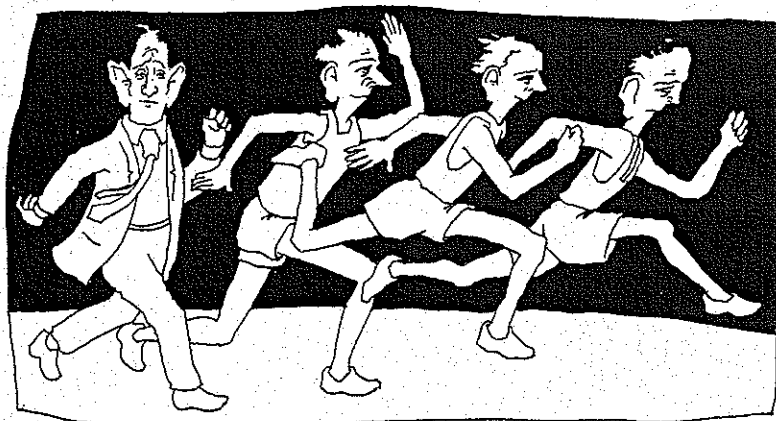
We have presented a discussion and comparison of bR thin film assemblies formed using several different immobilization methods. Oriented and biofunctional bR films may be obtained using each of the methods described. However, each method offers its own advantages and disadvantages. For example, LBL deposition is currently the simplest of all

the techniques and offers a high degree of orientation of the bR in the assemblies. In addition, LBL is versatile in that a wide variety of charged species may be easily intercalated with the bR to build in additional functionality. However, if thicker films are required, other techniques such as EFS or polymer encapsulation may be more suitable and can offer similar degrees of orientation. Fundamentally, the effect of azide on the photocurrents of WT-PM and D96N supports the mechanism that the differential light-on photocurrent originates mainly from the net proton release due to the formation of the M intermediate, and the light-off photocurrent originates from the net proton uptake due to the decay of M intermediate. Also, it has been shown that some bR mutants show enhanced photochemical and photophysical properties. All of these factors (practical and fundamental) are important and must be taken into consideration when one is designing a bR thin film assembly to suit a particular application.

Received: January 5, 1999

- [1] A. Ulman, *An Introduction to Ultrathin Organic Films: From Langmuir-Blodgett to Self-Assembly*, Academic, Boston, MA 1991. E. Sackmann, *Science* 1996, 271, 43.
- [2] M. C. Petty, *Langmuir-Blodgett Films: An Introduction*, Cambridge University Press, Cambridge 1996.
- [3] W. Müller, H. Ringsdorf, E. Rump, G. Wildburg, X. Zhang, L. Angelmaier, W. Knoll, M. Liley, J. Spinke, *Science* 1993, 262, 1706. K. Ng, D. W. Pack, D. Y. Sasaki, F. H. Arnold, *Langmuir* 1995, 11, 4048.
- [4] D. Oesterhelt, W. Stoerkenius, *Nature (London)*, *New Biol.* 1971, 233, 149. D. Oesterhelt, W. Stoerkenius, *Proc. Natl. Acad. Sci. USA* 1973, 70, 2853.
- [5] Y. Shen, C. R. Safinya, K. S. Liang, A. F. Ruppert, K. J. Rothschild, *Nature* 1993, 366, 48.
- [6] T. Miyasaka, K. Koyama, *Thin Solid Films* 1992, 210/211, 146. T. Furuno, K. Takimoto, T. Kouyama, A. Ikegami, H. Sasabe, *Thin Solid Films* 1988, 160, 145. M. Ikonen, J. Peltonen, E. Vuorimaa, H. Lemmetyinen, *Thin Solid Films* 1992, 213, 277. H. H. Weetall, L. A. Samuelson, *Thin Solid Films* 1998, 312, 306.
- [7] L. Keszthelyi, *Biochim. Biophys. Acta* 1980, 598, 429.
- [8] R. A. Brizzolara, *Biosystems* 1995, 35, 137. R. A. Brizzolara, B. C. Beard, *J. Vac. Sci. Technol. A* 1994, 12, 2981.
- [9] J.-A. He, L. Samuelson, L. Li, J. Kumar, S. K. Tripathy, *Langmuir* 1998, 14, 1674. J.-A. He, L. Samuelson, L. Li, J. Kumar, S. K. Tripathy, *J. Phys. Chem. B* 1998, 102, 7067.
- [10] K. Koyama, N. Yamaguchi, T. Miyasaka, *Science* 1994, 265, 762. K. Koyama, N. Yamaguchi, T. Miyasaka, *Adv. Mater.* 1995, 7, 590.
- [11] S. G. Wu, L. M. Ellerby, J. S. Cohan, B. Dunn, M. A. El-Sayed, J. S. Valentine, J. I. Zink, *Chem. Mater.* 1993, 5, 115. H. H. Weetall, *Appl. Biochem. Biotechnol.* 1994, 49, 241.
- [12] Z. Chen, A. Lewis, H. Takei, I. Nebenzahl, *Appl. Opt.* 1991, 30, 5188. Z. Chen, K. Chittibabu, K. Marx, J. Kumar, S. K. Tripathy, L. A. Samuelson, J. Akkara, D. L. Kaplan, *SPIE Proc.* 1994, 2189, 105.
- [13] A. Lewis, Y. Albeck, Z. Lange, J. Benchowski, G. Weizman, *Science* 1997, 275, 1462.
- [14] R. R. Birge, *Annu. Rev. Phys. Chem.* 1990, 41, 683.
- [15] J. K. Lanyi, *Biochim. Biophys. Acta* 1993, 1183, 241.
- [16] W. Stoerkenius, R. H. Lozier, R. A. Bolgomolnii, *Biochim. Biophys. Acta* 1979, 505, 215.
- [17] F. Gai, K. C. Hasson, J. C. McDonald, P. A. Anfirrud, *Science* 1998, 279, 1886. J. Tittor, C. Soell, D. Oesterhelt, H. J. Butt, E. Bamberg, *EMBO J.* 1989, 8, 3477. B. F. Ni, M. Chang, A. Duschl, J. Lanyi, R. Needleman, *Gene* 1990, 90, 169.
- [18] E. Pebay-Peyroula, G. Rummel, J. P. Rosenbusch, E. M. Landau, *Science* 1997, 277, 1676. H. Luecke, H.-T. Richter, J. K. Lanyi, *Science* 1998, 280, 1934. L. S. Brown, J. Sasaki, H. Kandori, A. Maeda, R. Needleman, J. K. Lanyi, *J. Biol. Chem.* 1995, 270, 27 122.
- [19] L. Zimányi, G. Váró, M. Chang, B. F. Ni, R. Needleman, J. K. Lanyi, *Biochemistry* 1992, 31, 8535. Y. Takeuchi, K. Ohno, M. Yoshida, K. Nagano, *Photochem. Photobiol.* 1981, 33, 587.

- [20] Z. P. Chen, R. R. Birge, *TIBTECH* 1993, 11, 292.
- [21] S. R. Caplan, G. Fischer, *J. Membr. Sci.* 1983, 16, 391.
- [22] A. R. McIntosh, F. Boucher, *Biochim. Biophys. Acta* 1991, 1056, 149. H.-W. Trissl, *Photochem. Photobiol.* 1990, 51, 793.
- [23] T. Miyasaka, K. Koyama, I. Otoh, *Science* 1992, 255, 342.
- [24] A. Popp, M. Wolperdinger, N. Hampp, C. Bräuchle, D. Oesterheld, *Biophys. J.* 1993, 65, 1449. M. Wolperdinger, N. Hampp, *Biophys. Chem.* 1995, 56, 189.
- [25] C. Bräuchle, N. Hampp, D. Oesterheld, *Adv. Mater.* 1991, 3, 420.
- [26] J. Y. Huang, A. Lewis, *Biophys. J.* 1989, 55, 835. J. Y. Huang, Z. P. Chen, A. Lewis, *J. Phys. Chem.* 1989, 93, 3314. R. R. Birge, M. B. Masthay, J. A. Stuart, J. R. Tallent, C.-F. Zhang, *Proc. SPIE* 1991, 1432, 129. Z. P. Chen, A. Lewis, J. Kumar, S. Tripathy, K. Marx, J. Akkara, D. Kaplan, *Mater. Res. Soc. Symp. Proc.* 1994, 330, 263.
- [27] R. J. Dunn, N. R. Hackett, J. M. McCoy, B. H. Chao, K. Kimura, H. G. Khorana, *J. Biol. Chem.* 1987, 262, 9246. M. Nassal, T. Mogi, S. S. Karnik, H. G. Khorana, *J. Biol. Chem.* 1987, 262, 9264.
- [28] R. H. Tredgold, *Order in Thin Organic Films*, Cambridge University Press, Cambridge 1994.
- [29] S.-B. Hwang, J. I. Korenbrot, W. Stoeckenius, *J. Membr. Biol.* 1977, 36, 115.
- [30] H. E.-M. Niemi, M. Ikonen, J. M. Levlin, H. Lemmetyinen, *Langmuir* 1993, 9, 2436.
- [31] S.-B. Hwang, J. I. Korenbrot, W. Stoeckenius, *J. Membr. Biol.* 1977, 36, 137. S.-B. Hwang, J. I. Korenbrot, W. Stoeckenius, *Biochim. Biophys. Acta* 1978, 509, 300.
- [32] N. Yamaguchi, Y. Jinbo, M. Arai, K. Koyama, *FEBS Lett.* 1993, 324, 287.
- [33] M. Kates, S. C. Kushwaha, G. D. Sprott, *Methods Enzymol.* 1982, 88, 98.
- [34] R. Jonas, Y. Koutalos, T. G. Ebrey, *Photochem. Photobiol.* 1990, 52, 1163.
- [35] U. Alexiev, T. Marti, M. P. Heyn, H. G. Khorana, P. Scherrer, *Biochemistry* 1994, 33, 298.
- [36] Y. Kimura, M. Fujiwara, A. Ikegami, *Biophys. J.* 1984, 45, 615.
- [37] J. P. Wang, S. K. Yoo, L. Song, M. A. El-Sayed, *J. Phys. Chem. B* 1997, 101, 3420. J. P. Wang, L. Song, S. K. Yoo, M. A. El-Sayed, *J. Phys. Chem. B* 1997, 101, 10599.
- [38] A. Dér, R. Tóth-Boconádi, L. Keszthelyi, H. Kramer, W. Stoeckenius, *FEBS Lett.* 1995, 377, 419.
- [39] G. Decher, *Science* 1997, 277, 1232.
- [40] G. Decher, J. D. Hong, J. Schmitt, *Thin Solid Films* 1992, 210/211, 831.
- [41] M. Ferreira, J. H. Cheung, M. F. Rubner, *Thin Solid Films* 1994, 244, 806. J. H. Cheung, M. Ferreira, M. F. Rubner, *Thin Solid Films* 1994, 244, 985.
- [42] M. Ferreira, M. F. Rubner, *Macromolecules* 1995, 28, 7107. S. Watanabe, S. L. Regan, *J. Am. Chem. Soc.* 1994, 116, 8855. S. Balasubramanian, X. G. Wang, H. C. Wang, K. Yang, J. Kumar, S. K. Tripathy, *Chem. Mater.* 1998, 10, 1554. A. C. Fou, O. Onitsuka, M. Ferreira, M. F. Rubner, B. R. Hsieh, *J. Appl. Phys.* 1996, 79, 7501.
- [43] Y. Lvov, K. Ariga, M. Onda, I. Ichinose, T. Kunitake, *Langmuir* 1997, 13, 6195. J. H. Fendler, *Chem. Mater.* 1996, 8, 1616. S. K. Tripathy, H. Katagi, H. Kasai, S. Balasubramanian, H. Oshikiri, J. Kumar, H. Oikawa, S. Okada, H. Nakanishi, *Jpn. J. Appl. Phys.* 1998, 37, L343.
- [44] K. Ariga, Y. Lvov, T. Kunitake, *J. Am. Chem. Soc.* 1997, 119, 2224. M. M. Fang, D. M. Kaschak, A. C. Sutorik, T. E. Mallouk, *J. Am. Chem. Soc.* 1997, 119, 12184.
- [45] F. Caruso, K. Niikura, D. N. Furlong, Y. Okahata, *Langmuir* 1997, 13, 3427. Y. Lvov, K. Ariga, I. Ichinose, T. Kunitake, *J. Am. Chem. Soc.* 1995, 117, 6117. M. Onda, Y. Lvov, K. Ariga, T. Kunitake, *Biotechnol. Bioeng.* 1996, 51, 163. Y. Lvov, G. Decher, G. Sukhorukov, *Macromolecules* 1993, 26, 5396. Y. Lvov, J. Haas, G. Decher, H. Möhwald, A. Mikhailov, B. Mchedlishvily, E. Morgunova, *Langmuir* 1994, 10, 4232.
- [46] C. Gergely, L. Zimányi, G. Váró, *J. Phys. Chem. B* 1997, 101, 9390.
- [47] Y. Lvov, K. Ariga, I. Ichinose, T. Kunitake, *Thin Solid Films* 1996, 284/285, 797. F. Caruso, D. N. Furlong, K. Ariga, I. Ichinose, T. Kunitake, *Langmuir* 1998, 14, 4559.
- [48] D. Q. Li, M. A. Ratner, T. J. Marks, C. H. Zhang, J. Yang, G. K. Wong, *J. Am. Chem. Soc.* 1990, 112, 7389.
- [49] O. Bouevitch, A. Lewis, *Opt. Commun.* 1995, 116, 170.
- [50] H.-W. Trissl, W. Gärtner, *Biophys. J.* 1987, 26, 751. L. Keszthelyi, P. Ormos, *Biophys. Chem.* 1983, 18, 397.
- [51] S. Y. Liu, *Biophys. J.* 1990, 57, 943.
- [52] S. Y. Liu, T. G. Ebrey, *Biophys. J.* 1988, 54, 321.
- [53] B. Robertson, E. P. Lukashov, *Biophys. J.* 1995, 68, 1507.
- [54] H. J. Butt, K. Fendler, E. Bamberg, J. Tittor, D. Oesterheld, *EMBO J.* 1989, 8, 1657. A. Miller, D. Oesterheld, *Biochim. Biophys. Acta* 1990, 1020, 57.
- [55] J. LeCoutre, J. Tittor, D. Oesterheld, K. Gerwert, *Proc. Natl. Acad. Sci. USA* 1995, 92, 4962. L. A. Drachev, A. D. Kaulen, A. Y. Komrakov, *FEBS Lett.* 1992, 313, 248.



Race ahead – subscribe to Advanced Materials.
See p. 431 for ordering information.